24th COBEM - 2017

24th ABCM International Congress of Mechanical Engineering
December 3-8, 2017, Curitiba, PR, Brazil

COBEM-2017-0219
A FUEL-AND-PRODUCT MODEL OF CONCENTRATING SOLAR POWER SYSTEMS FOR APPLICATION IN EXERGY ANALYSIS

Thiago de Oliveira Macedo[1]
Manuel Ernani de Carvalho Cruz[2]
Universidade Federal do Rio de Janeiro – UFRJ
Programa de Engenharia Mecânica – COPPE
CP 68503, Centro de Tecnologia – CT, Cidade Universitária, Rio de Janeiro, RJ
CEP: 21941-972
[1]thiagomacedo@mecanica.coppe.ufrj.br, [2]manuel@mecanica.coppe.ufrj.br

Leonardo dos Santos Reis Vieira[3]
Centro de Pesquisas de Energia Elétrica – CEPEL
Departamento de Tecnologias Especiais – DTE
Cidade Universitária, Rio de Janeiro, RJ
CEP: 21941-911
[3]lsrv@cepel.br

Abstract. *Exergy-based methodologies applicable to energy conversion systems have undergone increased development in academia. Currently these methodologies consider different possibilities of combination of thermodynamic, economic and environmental aspects, and they are classified into conventional or advanced. The results generated by these methodologies may be conveniently utilized to direct optimization or improvement procedures of energy conversion systems. The exergy balance is the supporting structure for these methodologies, and the concepts of Fuel and Product proposed in the literature permit rewriting the exergy balance for the different components of an energy conversion system in a simple and useful form. The increased interest in new sources of energy, in a context of coexistence of increased energy demand and the quest for sustainability, naturally results in the development of new technologies. These technologies might hinder the direct application of the concepts of Fuel and Product to a given component, as well as hinder the identification and calculation of exergy associated with a given component flux. In the present work, a Fuel-and-Product model is proposed to represent a solar field with parabolic collectors, that are part of a concentrating solar power plant. Four formulations for exergy calculation associated with the solar radiation are utilized in the proposed model. The results show different amounts of exergy destruction, which may be relevant to direct optimization or improvement procedures of the solar plant as a whole, from the thermodynamic viewpoint.*

Keywords: *concentrating solar power, fuel and product, exergy, solar radiation, concentrated solar power plant*

1. INTRODUCTION

The concentrating solar power (CSP) systems are, essentially, of four types: Fresnel, Tower, Parabolic Dish, or Parabolic Trough. For these systems, recent studies based on the concept of exergy are available in the literature. For example, Xu *et al.* (2011) and Reddy *et al.* (2013) conducted an exergy analysis, respectively, of a tower and a dish system. The exergetic analysis was applied to parabolic trough systems by Mahfuz *et al.* (2014) integrated to a Rankine cycle, and by Al-Sulaiman (2014) integrated to combined cycles. Nixon and Davies (2012) used the concept of exergy to optimize Fresnel systems. More recently, Cavalcanti (2017) performed the exergoeconomic and exergoenvironmental analyses of a parabolic trough system integrated to a gas-vapor combined cycle. Still, for CSP systems, it is apparent that not many exergy-based methodologies are available for analysis, improvement or optimization.

In the aforementioned works and in others associated with solar fields with technologies for concentration, it is not possible to identify a formal and clear definition of the concepts of Fuel and Product in the form they were originally proposed by Tsatsaronis (Lazzaretto and Tsatsaronis, 1999). The application of these exergy-based concepts has contributed to the analysis, optimization (Bejan *et al.*, 1996) and improvement (Vieira *et al.*, 2009) of many different thermal systems, including aspects relating to cost and environmental impact. However, the application of the Fuel and Product concepts to CSP systems is still in need of development. To that effect, it is necessary to estimate the exergy

associated with solar radiation. Although some formulations do exist in the literature to estimate the solar radiation exergy, they are based on different hypotheses. Furthermore, there seems to be no systematic comparison of these formulations with a view to application to CSP systems.

The objective of the present work is to propose a Fuel-and-Product model appropriate for application to exergy analyses of CSP systems. The model employs the four more widespread formulations to estimate the exergy associated with solar radiation. A critical comparison of the ensuing results is also effected in the light of solar systems applications.

2. PROPOSED MODEL

Basically, each of the four types of CSP systems consists of two sub-systems: the optical sub-system, comprising the set of concentrating mirrors, and the absorbing sub-system, comprising an absorbing surface or an absorbing pipe. The optical sub-system is responsible for directing the solar radiation to the absorbing sub-system, through which a thermal fluid circulates. The fluid may have different compositions, for example, mineral oils, synthetic oils, and molten salt. At the collector exit, the heated thermal fluid supplies the necessary thermal energy to a conventional steam power plant. The proposed Fuel-and-Product model, based on the exergy fluxes shown in Fig. 1, shall be applicable to all four types of existing CSP systems.

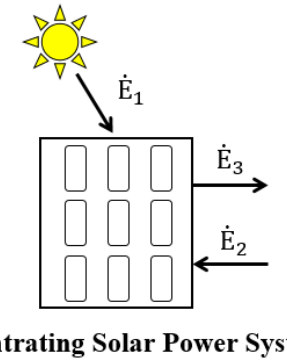

Figure 1. Diagram for the proposed Fuel-and-Product model for CSP systems

The model represents a CSP solar field, where the exergy fluxes $\dot{E}_1$, $\dot{E}_2$, and $\dot{E}_3$ denote, respectively, solar radiation input, thermal fluid inlet, and thermal fluid outlet. The flux $\dot{E}_1$ is discontinuous, and is related to the exergy of the solar field incident radiation. The fluxes $\dot{E}_2$ and $\dot{E}_3$ are considered continuous, and are related to the exergy of the thermal fluid, respectively, at the entrance and exit of the solar field. Accordingly, Fuel is the solar radiation input to the field, $\dot{E}_1$, and Product is the increment in exergy of the thermal fluid between the entrance and exit of the field, $\dot{E}_3 - \dot{E}_2$. In terms of exergy, the proposed Fuel-and-Product model is similar to the model of a rotating machine as put forth by Tsatsaronis (Bejan *et al*., 1996).

The fluxes $\dot{E}_2$ and $\dot{E}_3$ represent transfer of exergy by mass flow. Each flux is calculated by the product of the respective mass flowrate and physical exergy of the stream, the latter given by

$$e = (h - h_0) - T_0(s - s_0) \tag{1}$$

In Eq. (1), h and s represent, respectively, the specific enthalpy and specific entropy in the state of interest, and h_0 and s_0 represent the same properties in the restricted dead state at temperature T_0 and pressure P_0. In this case, the variations in kinetic and potential exergies are neglected. In addition, it is considered that the thermal fluid operates within the recommended temperature range, such that it remains in the liquid phase, and does not degrade through chemical reactions. Thus, the composition of the thermal fluid is invariable, such that the chemical exergy does not change between the states of interest.

There exist different standpoints in the literature regarding the calculation of the energy and exergy associated with the flux $\dot{E}_1$. In the present work, the flux $\dot{E}_1$ is calculated by the expression

$$\dot{E}_1 = \eta \times R \times A_f \tag{2}$$

In Eq. (2), η, R, and A_f represent, respectively, the efficiency factor of the formulation for the exergy associated with solar radiation (non-dimensional), the amount of direct solar irradiance (kW/m^2), and the aperture area of the solar field (m^2). The determination of R is presented in section 3.1, and the calculation of η is presented in section 3.2.

The exergy balance for this system (Bejan *et al*., 1996) can be expressed by

$$\dot{E}_P = \dot{E}_F - (\dot{E}_D + \dot{E}_L) \tag{3}$$

In Eq. (3), $\dot{E}_P$, $\dot{E}_F$, $\dot{E}_D$ and $\dot{E}_L$ represent, respectively, the Product rate, the Fuel rate, the rate of exergy destruction and the rate of exergy loss. Thus, the sum $\dot{E}_D$+ $\dot{E}_L$ represents the portion of fuel exergy not converted into product exergy. As a consequence, the decrease of $\dot{E}_D$+ $\dot{E}_L$ (or increase of $\dot{E}_P$) is related to the exergetic efficiency (ε) increase. It should be noted that the portion $\dot{E}_L$ is not destroyed in the energy conversion process taking place in the system. The portion $\dot{E}_L$ embodies the exergy escaped from the process. For a conveniently chosen system boundary at ambient temperature T_0, $\dot{E}_L$ = 0 and, consequently, all the portion of fuel exergy not converted into product exergy is the system´s exergy destruction, $\dot{E}_D$.

In the proposed Fuel and Product model, the portion of Fuel not converted to Product is related to the optical and thermal performances of the solar field. The amount of incident energy on a collector is reduced depending on the solar incidence angle and several other factors related to the collector design. This reduction is accounted for by the optical performance of the solar field. In addition, the process of capturing solar radiation results in an increase of the operating temperature of the collector to values above the ambient temperature. This temperature difference, in turn, results in thermal losses by conduction, convection and radiation, accounted for by the thermal performance of the solar field. In general, losses by convection and radiation are dominant.

To evaluate the performance of the solar field with respect to the degradation of energy, it is necessary to conceive an ideal reference model process for the energy conversion taking place. The ideal process is here denoted ideal thermal absorption process, in which all the direct radiation energy is absorbed by the thermal fluid as it passes through the solar field. For a solar field operating in steady-state, the thermal fluid state at the entrance and the pressure at the exit are fixed. Applying the energy balance to the solar field in Fig. 1, the absorbed energy is equal to the difference in enthalpy of the thermal fluid between the entrance and exit of the field, since there is no work interaction, and the variations in kinetic and potential energies are neglected. A conversion efficiency can, therefore, be defined, denoted thermal absorption efficiency τ, as the ratio of the absorbed energy in a real process and the absorbed energy in the ideal process, such that

$$\tau = \frac{h_{3r} - h_{2r}}{h_{3s} - h_{2s}} \tag{4}$$

In Eq. (4), h represents the thermal fluid specific enthalpy, the stations 2 and 3 designate, respectively, the entrance and exit of the solar field, and the subscripts s and r designate, respectively, ideal process and real process. The energy absorbed in the real process is smaller than the energy absorbed in the ideal process. To calculate the thermal absorption efficiency, it is considered that $h_{2s} = h_{2r}$.

3. SOLAR RADIATION

3.1 Energy associated with solar radiation in CSP systems

The Sun is essentially a nuclear reactor, where the generated energy comes from the continuous fusion reaction during which two hydrogen atoms fuse into a helium atom. The solar energy that reaches the Earth´s atmosphere is denoted total irradiance and its estimated value is 1373 W/m^2 (Çengel and Ghajar, 2011). The value of the total irradiance can be used to estimate the superficial effective temperature of the Sun, which results in 5780 K. Solar radiation is considerably attenuated as it crosses the terrestrial atmosphere, the region within 30 km from the Earth´s surface, due to absorption and scattering. These phenomena originate from the influence of some gases and particles present in the atmosphere. As a result, the value of solar power that reaches the terrestrial surface decreases to about 950 W/m^2 and even to much lower values in cloudy days or in locations with elevated pollution levels (Çengel and Ghajar, 2011).

The global energy associated with the incident solar radiation on the horizontal terrestrial surface is made up of the direct and diffused (scattered) components. However, the direct component is reduced proportionally to the cosine of the angle of incidence, the angle that the Sun rays form with the surface normal. In addition to global solar radiation, the terrestrial surface is also subject to the incidence of atmospheric radiation, diffuse in character, emitted by molecules of gases and particles suspended in the atmosphere. Therefore, the total radiation incident on the horizontal terrestrial surface is equal to the sum of the global solar radiation and the atmospheric radiation. However, given that it is not possible to focus the diffuse radiation, only the energy associated with the direct incident solar radiation is considered for the concentrating systems in the present work.

3.2 Exergy associated with solar radiation in CSP systems

In the past, studies related to the ideal conversion process for thermal radiation developed based on different approaches. The first approach considered a blackbody radiation at a certain temperature as the thermodynamic system.

The analysis concentrated on the estimation of the maximum work possible of being performed by the system until it reached the dead state, the condition of equilibrium between the system and environment (Petela, 1964; Spanner, 1964; Jeter, 1981; Parrott, 1978). The second approach, in its turn, concentrated on the estimation of the maximum work possible of being performed by diverse thermal and quantum conversion devices (De Vos, 1992).

To simplify, the present work considers the formulations related to the first approach to calculate the exergy associated with thermal radiation. In this approach, thermal radiation is modeled as blackbody radiation. Since the behavior of solar radiation is closely approximated by blackbody radiation, the formulations can be applied to the direct solar radiation. Tab. 1 summarizes the four formulations to calculate the direct solar radiation exergy employed in this work. These formulations have been analyzed by several different authors (Petela, 2003; Wright *et al.*, 2002; Bejan, 1987). Table 1 informs the year of development and a brief description of the characteristics and adopted hypotheses for each formulation. In the table, the efficiency factor η is the ratio of the exergy flux associated with solar radiation and the energy flux of direct solar radiation.

Table 1. Formulations to calculate the exergy associated with direct solar radiation.

Formulation	Efficiency factor, η	Year	Description
Petela	$1+\frac{1}{3}\left(\frac{T_0}{T}\right)^4-\frac{4}{3}\frac{T_0}{T}$	1964	To calculate the maximum useful work performed by the system, an adiabatic piston-cylinder apparatus is considered, with perfectly mirrored walls and piston base. Inside, there is blackbody radiation at temperature T. The ambient is formed by blackbody radiation in vacuum at temperature T_0. When analyzing the exergy of the direct solar radiation, Press (1976) obtained the same results as Petela.
Spanner	$1-\frac{4}{3}\frac{T_0}{T}$	1964	The derived expression is termed maximum economic efficiency. As opposed to Petela (1964), Spanner considers the absolute work, rather than the useful work. The difference between them is the work against the environment until the equilibrium between system and environment is reached. The absolute temperatures associated with radiation at the beginning and end of the process are T and T_0, respectively.
Jeter	$1-\frac{T_0}{T}$	1981	Jeter considers a thermal engine in direct contact with the Sun (source, reservoir at temperature T) and the Earth (sink, reservoir at temperature T_0).
Parrott	$1+\frac{1}{3}\left(\frac{T_0}{T}\right)^4-\frac{4}{3}\frac{T_0}{T}(1-\cos(\delta))^{\frac{1}{4}}$	1978	Parrott considers a clear day and the cone angle subtended by the Sun; δ represents half of this angle. The angle δ is 0.0047 rad. As opposed to Petela (1964), Parrott considers the dependence of the propagation of radiation according to its direction. For δ equal to 1.57 rad ($\approx 90°$), the expression by Parrott becomes identical to the expression by Petela.

To apply the formulations in the proposed Fuel-and-Product model, the effective superficial temperature of the Sun is considered T = 5780 K. The ambient temperature is T_0, used as the reference for exergy calculation. In the application of Parrott's formulation, the value of 0.0047 has been considered for the angle δ.

4. METHODOLOGY

The modeling and simulation of the solar field have been carried out with the IPSEpro® 6.0 process simulator (SimTech, 2013), using the PSE module (Process Simulation Environment). The MDK module (Model Development Kit) is used for building a new library, based on the original library CSP_Lib (Concentrating Solar Power Library). The new library computes the exergies of the various streams of the system, including the exergy associated with solar radiation according to the four formulations described in Tab. 1. Because the entropy of the thermal fluid is not available in the CSP_Lib, the physical exergies of the thermal fluid streams are determined by first computing the entropy of the thermal fluid using the C++ library CoolProp® (CoolProp, 2017). Thus, the implementation of the exergy analysis has been realized within the MatLab environment (Gilat, 2014), integrated with the IPSEpro process simulator and the CoolProp® library. MatLab receives from IPSEpro the values of the mass and energy balances, exchanges data with CoolProp to calculate the physical exergy of the thermal fluid, and effects the computations of the exergy analysis itself. The

parametric analyses have also been implemented within the MatLab environment. The interface IPSEpro-MatLab uses the COM type interface (Component Object Model) by Microsoft® (Microsoft, 2017). The interface MatLab-CoolProp has been performed through high level calls to CoolProp from MatLab.

The modeling and simulation of the solar field in IPSEpro is shown in Fig. 2. The configuration of the solar field in the IPSEpro program is relatively simple. The following set of input data is necessary: the thermodynamic properties of the fluids at the entrance and exit of the solar field, the direct solar radiation, the day of the year, the hour of the day, the latitude, the pressure and temperature of the ambient, and the relative humidity. All the other variables are calculated in the simulation, including the optical and thermal losses in the solar field. The losses depend on the design of the solar collector chosen for simulation.

The present methodology is applied to three cases, designated as Case 1, Case 2, and Case 3. Case 1 consists in the comparison of the efficiency factor from the formulations by Petela, Spanner, Jeter and Parrott (Tab. 1). Case 1 has been realized in two steps. In the first step of Case 1, for a fixed value of T_0, T_0 = 298.15 K (25°C), η is evaluated for T between 298.15 K (25°C) and 6000 K (5726.85°C). In the second step of Case 1, for a fixed value of T, T = 5780 K (5506.85°C), η is evaluated for T_0 between 298.15 K (25°C) and 323.15 K (50°C).

Case 2 consists in a conventional exergy analysis of a solar field, using the formulations by Petela, Spanner, Jeter and Parrott. The solar field is considered to be in steady-state in the location of Petrolina, PE, Brazil. The solar field is composed of three loops, with four parabolic trough collectors per loop. The thermal fluid is the Therminol VP-1® (Therminol, 2017) oil. A pump drives the thermal fluid between the entrance and exit of the field. For a given aperture area of the solar field and a fixed value of the direct solar radiation, Fuel is a function of η only. The state of the thermal fluid at the entrance of the solar field and the exit pressure are fixed. In this manner, T_2 = 200°C, P_2 = 12.5 bar, $\dot{m}_2$ = 10 kg/s and $P_3 = P_2$, where T, P and $\dot{m}$ represent, respectively, temperature, pressure and mass flow rate of the thermal fluid, and the subscripts 2 and 3 indicate, respectively, the entrance and exit of the field. In these conditions, for constant Fuel rates, the rates of Product and exergy destruction depend on the design of the collector.

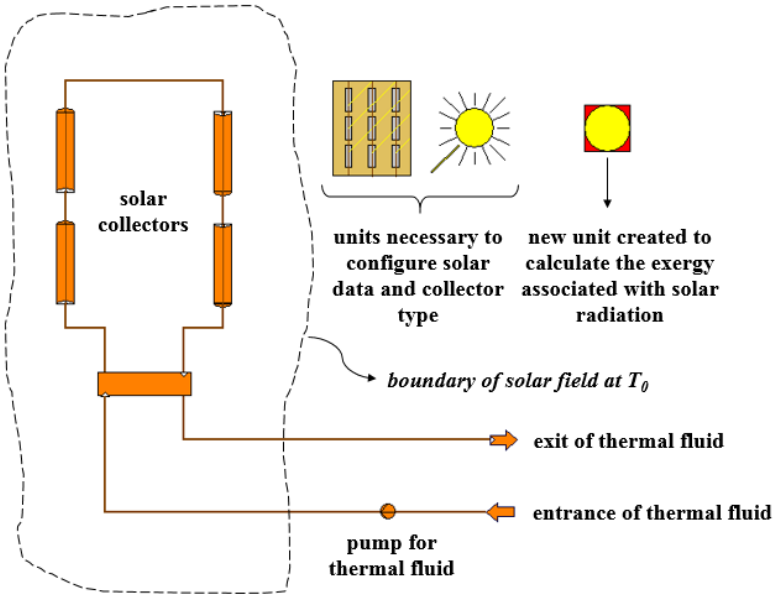

Figure 2. Modeling and simulation of the solar field in IPSEpro environment for Cases 2 and 3

Meteorological data from 2007 to 2010 at the Petrolina airport have been used according to the SWERA (Solar and Wind Energy Resource Assessment, https://maps.nrel.gov/swera) model (CEPEL, 2012) . The period with the most solar incidence, between September 05 and November 16, has been identified with the help of the WeatherSpark system (Cedar Lake Ventures, 2017). The data of the WeatherSpark system are based on statistical analyses of satellite measurements between 1980 and 2016. In the period between September 05 and November 16, October 11 is a clear day with the highest level of global solar radiation. In addition, the highest level of direct solar irradiance is also on October 11, at 12:00 h, with a value of 0.895 kW/m^2. This is the irradiance value for Case 2. Two commercial models of collectors, C1 and C2, with the same aperture area are used to compare the behavior of two different solar fields. Solar Field A is composed of collectors of model C1, and Solar Field B is composed of collectors of model C2. In both fields, the aperture area is 4578 m^2.

Case 3 consists in a conventional exergy analysis of Solar Field A along the day October 11 between 07:00 h and 17:00 h. For Case 3, the same meteorological data from Case 2 have been used. The entrance and exit states are fixed as follows: T_2 = 40°C, P_2 = 12.5 bar, T_3 = 390°C, $P_3 = P_2$. Finally, in Case 3, the variable mass flow rate is calculated for each hour of the day between 07:00 h and 17:00 h.

5. RESULTS AND DISCUSSION

Figure 3 presents the results for the first step of Case 1. For the entire range of temperature T of the emitting body surface, it is possible to observe that the behavior of the Parrott formulation is significantly different when compared to the behavior of the other formulations. For the temperature T varying from 298.15 K (25°C) to approximately 1800 K (1526.85°C), keeping T_0 constant at 298.15 K (25°C), the efficiency factor for the Petela, Spanner and Jeter formulations shows a rapid increase. Besides, for the entire range of T analyzed, the efficiency factor increases as T increases. On the other hand, for the Parrott formulation, the efficiency factor decreases until T reaches approximately 500 K, and remains nearly constant between 500 K (226.85°C) and 6000 K (5726°C). Also, for the entire range of T analyzed, the Parrott formulation yields a higher value for the efficiency factor compared to the other formulations. For Parrott, when T is close to T_0, 298.15 K $\leq T \leq$ 500 K, the term $1/3(T_0/T)^4$ grows more rapidly than the term $4/3(T_0/T)(1 - \cos(\delta))^{1/4}$ and, consequently, the efficiency factor takes on values greater than unity. When T grows away from T_0, i.e., $T >$ 500 K, the inverse trend occurs, the term $4/3(T_0/T)(1 - \cos(\delta))^{1/4}$ grows more rapidly than the term $1/3(T_0/T)^4$, and the efficiency factor takes on values smaller than unity.

Negative values of the efficiency factor are observed only for the Spanner formulation. The negative value resulting from $T = T_0$ has no physical significance, since $T = T_0$ represents a condition of equilibrium between the system of interest and the ambient. Therefore, the exergy associated with irradiance must be null. The other negative values (for T not equal to T_0) of the efficiency factor (and also the positive values) are due to the condition of non-equilibrium between the system and ambient, what results in a potential for doing useful work (nonzero exergy). The null value of the efficiency factor means, physically, the absence of interaction between the system of interest and the ambient, in addition to the impossibility of spontaneous changes in the two systems considered. The formulations by Petela and Spanner exhibit very similar behaviors throughout most of the range of T. In this work, for the temperature of interest to be used in the proposed Fuel-and-Product model, T = 5780 K, the formulations by Petela, Spanner, Jeter and Parrott result in efficiency factors equal to, respectively, 0.9300, 0.9300, 0.9475 and 0.9960. The efficiency factor of the Jeter formulation is equal to the Carnot factor $(1 - T_0/T)$. Therefore, the formulations by Petela, Spanner and Parrott deviate from the behavior of the Carnot engine.

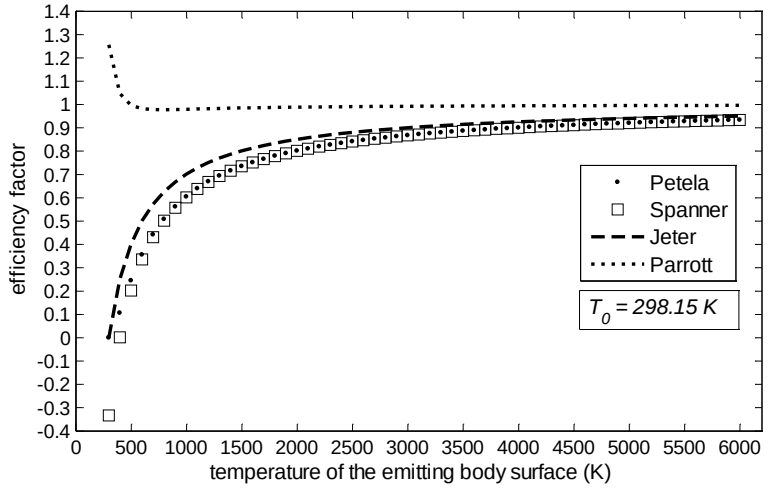

Figure 3. Comparison of the efficiency factor for the four formulations, 298.15 K $\leq T \leq$ 6000 K, T_0 = 298.15 K

Figure 4 presents the results for the second step of Case 1, in which the blackbody temperature (T = 5780K) is kept fixed. For the Petela, Spanner and Jeter formulations, it is possible to observe a smooth decrease in the efficiency factor as the temperature T_0 increases. The efficiency factor for the Parrott formulation is approximately constant. It is noteworthy that the Petela and Spanner formulations lead to congruent values within the entire range of ambient temperature analyzed.

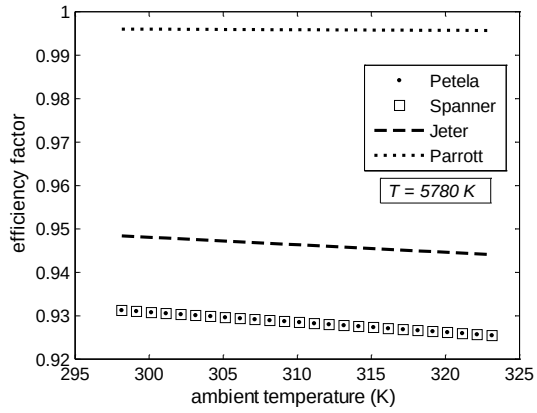

Figure 4. Comparison of the efficiency factor for the four formulations, 298.15 K ≤ T_0 ≤ 323.15 K, T = 5780 K

Tables 2 and 3 present the results for Case 2, for Solar Fields A and B, respectively. Solar field Product is related to the collector design and is independent of the formulation considered. For Solar Field A, Product flow rate is 2630.19 kW. For all formulations, the thermal fluid absorbs the same amount of energy, and leaves the solar field at 326.1°C. On the other hand, for a given aperture area and level of direct solar radiation, Fuel flow rate is a function of the efficiency factor. In this way, the Fuel flow rates increase as the efficiency factor increases, which results in larger exergy destruction rates for the same Product flow rate. Thus, for the Solar Field A, the Parrott formulation leads to the largest value of exergy destruction (1450.59 kW), followed by the Jeter formulation (1251.94 kW) and then by the Petela and Spanner formulations (1180.2 kW). The essentially identical results obtained with the Petela and Spanner formulations reflect the fact that the efficiency factor is also approximately the same for both formulations. Similar observations can also be stated for Solar Field B, based on the values shown in Tab. 3.

The Fuel flow rates are the same for each formulation for both Solar Fields A and B, because both fields have the same aperture area and are subjected to the same level of direct solar radiation. Thus, the values of Fuel flow rates for the Petela, Spanner, Jeter and Parrott formulations are equal to, respectively, 3810.4 kW, 3810.4 kW, 3882.1 kW and 4080.8 kW, independently of the chosen type of collector.

For a given formulation, a larger value of exergy destruction (or lower value of exergetic efficiency) is observed in Solar Field B. For Parrott formulation, for example, the Solar Fields A and B exergetic efficiencies are equal to 64.45% and 62.67%, respectively, and exergy destruction in Solar Field B is 72.9 kW higher than in Solar Field A. These results are related to the design of the collectors, such that, in Solar Field B, the thermal fluid absorbs a smaller amount of energy. As a consequence, in Solar Field B, the fluid reaches a final lower temperature (322.9°C) in comparison to Solar Field A (326.1°C).

It is possible to associate the value of exergy destruction to the thermal absorption efficiency τ. Solar Field A presents a larger value of thermal absorption efficiency, 68.32%, as compared to Solar Field B, 66.44%. The physical meaning of this result is that Solar Field A better approximates the ideal thermal absorption process, leading, therefore, to a lower value of exergy destruction. This fact is reflected in a higher thermal fluid ideal exit temperature (T_{3s}) compared to the thermal fluid real exit temperature (T_{3r}) for both fields. In this sense, the thermal absorption efficiency represents a simplified indication of the thermal and optical performances of the solar field. These performances are generally expressed by complex relations inherent to each specific type of collector.

In summary, for the same operational conditions, a solar field with a relatively higher thermal absorption efficiency results in a larger amount of energy absorption and, therefore, in a higher exit temperature of the thermal fluid, and less exergy destruction. Case 2 reveals distinct values of the exergy destruction for the three formulations by Petela, Jeter and Parrott. The same value is obtained for the Petela and Spanner formulations. The smallest exergy destruction occurs for Solar Field A with Petela and Spanner formulations, while the largest exergy destruction occurs for Solar Field B with Parrott formulation.

Table 2. Results for Case 2 for Solar Field A.

Formulation	$\dot{E}_F$ (kW)	$\dot{E}_P$ (kW)	$\dot{E}_D$ (kW)	ε (%)	η	h_{2s}=h_{2r} (kJ/kg)	h_{3s} (kJ/kg)	h_{3r} (kJ/kg)	T_{3s} (°C)	T_{3r} (°C)	τ (%)
Petela	3810.4	2630.2	1180.2	69.03	0.9300	355.3	765.0	635.2	378.9	326.1	68.32
Spanner	3810.4	2630.2	1180.2	69.03	0.9300	355.3	765.0	635.2	378.9	326.1	68.32
Jeter	3882.1	2630.2	1251.9	67.75	0.9475	355.3	765.0	635.2	378.9	326.1	68.32
Parrott	4080.8	2630.2	1450.6	64.45	0.9960	355.3	765.0	635.2	378.9	326.1	68.32

Table 3. Results for Case 2 for Solar Field B.

Formulation	$\dot{E}_F$ (kW)	$\dot{E}_P$ (kW)	$\dot{E}_D$ (kW)	ε (%)	η	$h_{2s} = h_{2r}$ (kJ/kg)	h_{3s} (kJ/kg)	h_{3r} (kJ/kg)	T_{3s} (°C)	T_{3r} (°C)	τ (%)
Petela	3810.4	2557.3	1253.2	67.11	0.9300	355.3	765.0	627.5	378.9	322.9	66.44
Spanner	3810.4	2557.3	1253.2	67.11	0.9300	355.3	765.0	627.5	378.9	322.9	66.44
Jeter	3882.1	2557.3	1324.9	65.87	0.9475	355.3	765.0	627.5	378.9	322.9	66.44
Parrott	4080.8	2557.3	1523.5	62.67	0.9960	355.3	765.0	627.5	378.9	322.9	66.44

As previously mentioned, Case 3 consists in a conventional exergy analysis of Solar Field A along October 11 between 07:00 h and 17:00 h. Table 4 shows the irradiance, the ambient temperature and the relative humidity ϕ along this period.

Table 4. Meteorological data according to the SWERA model for Case 3.

Hour of the day	*Irradiance* (kW/m^2)	T_0 (°C)	ϕ (%)
07:00	0.491	23.9	67
08:00	0.550	25.2	61
09:00	0.670	26.5	56
10:00	0.806	27.8	51
11:00	0.866	29.1	47
12:00	0.895	30.4	43
13:00	0.882	30.7	41
14:00	0.894	30.9	39
15:00	0.867	31.2	37
16:00	0.812	31.5	35
17:00	0.505	31.7	34

Day of the year: 284
Latitude: -9.362°
Collector C1 – design data according to Herrmann/Nava "Performance of the SKAL-ET Collectors of the Andasol Power Plants" 14th SolarPACES-Symposium 2008 (SimTech, 2013).

Figure 5 presents the results for Case 3, where it is possible to observe the distribution of exergy destruction for the Solar Field A along the day for the four evaluated formulations. For all formulations, it is possible to note a peak in the exergy destruction flow rate at 12:00 h for irradiance equal to 0.895 kW/m^2 and T_0 = 30.4°C. For all formulations, the smallest value of exergy destruction occurs at 08:00 h, when the irradiance equals to 0.550 kW/m^2 and T_0 = 25.2°C. During the whole day, the formulations by Petela and Spanner provide the same exergy destruction flow rates. This result is consistent with the findings from Case 1, where a close behavior of the Petela and Spanner formulations has been observed for a wide range of T_0.

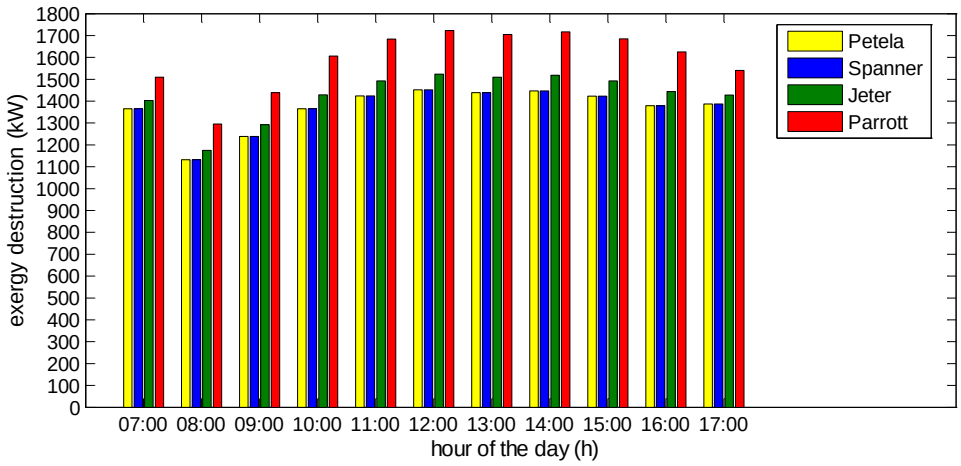

Figure 5. Distribution of exergy destruction in the course of the day hours according to Case 3

The exergy destruction flow rates depend not only on the radiation conditions, but also on the ambient conditions. The lowest irradiance level is observed at 07:00 h, however, this hour does not correspond to the smallest exergy destruction. In fact, as indicated in Fig. 5, the exergy destruction flow rates at the hours of 08:00 h and 09:00 h are smaller than that at 07:00 h, in spite of the larger irradiance at those hours relative to that at 07:00 h. Therefore, it is observed that the hourly values of exergy destruction are not readily predicted.

For Case 3, it is observed that the formulation by Parrott results in larger exergy destruction flow rates for all hours. However, the deviations of the Parrott formulation with respect to the other three vary in magnitude depending on the hour considered.

6. CONCLUSIONS

In the present work, a Fuel-and-Product model is proposed to represent a solar field with parabolic collectors, that are part of a concentrated solar power plant. The model is appropriate for exergy analyses of CSP systems. In this model, Fuel is identified with the exergy associated with the direct solar radiation. Product is identified with the increment in exergy of the thermal fluid between the entrance and exit of the solar field. To calculate the exergy flux associated with solar radiation, it has been necessary to identify the energy of the solar radiation that is effectively used. The exergy flux is determined based on four formulations available in the literature (Petela, Spanner, Jeter and Parrott). The formulations have been compared through the application of the proposed model to a reference CSP plant designed for operation at the location of Petrolina, PE, Brazil.

The proposed Fuel-and-Product model leads to results that are compatible with the engineering reality of CSP systems. For the same operational conditions of engineering interest, the formulations by Petela and Spanner result in the same value of exergy destruction in the solar field, and distinct from those obtained with the Jeter and Parrott formulations.

It is also verified that the exergy destruction depends not only on the radiation conditions, but also on the ambient conditions. For example, in the course of one day, the hour of least exergy destruction not always corresponds to the hour of least solar incidence.

For future work, it is suggested that the proposed Fuel-and-Product model be used as part of methodologies for analysis, optimization and improvement of energy conversion systems, in particular, with a view for application to CSP systems.

7. ACKNOWLEDGEMENTS

M.E.Cruz thanks the support provided by CNPq-Brazilian National Council for Scientific and Technological Development (Grant no. 303208/2014-7).

8. REFERENCES

Al-Sulaiman, F. A., 2014. “Exergy analysis of parabolic trough solar collectors integrated with combined steam and organic Rankine cycles”. *Energy Conversion and Management*, Vol. 77, pp. 441-449.

Bejan, A., 1987. “Unification of Three Different Theories Concerning the Ideal Conversion of Enclosed Radiation”. Trans. ASME, *Journal of Solar Energy Engineering*, Vol. 109, pp. 46-51.Cavalcanti, E. J. C., 2017. “Exergoeconomic and exergoenvironmental analyses of an integrated solar combined cycle system”. *Renewable and Sustainable Energy Reviews*, Vol. 67, pp. 507-519.

Bejan, A., Tsatsaronis, G. and Moran, M., 1996. *Thermal Design and Optimization*. John Wiley & Sons, New York, 1st edition.

Cedar Lake Ventures Inc., 2017. “WeatherSpark 1980-2016 Average Weather at Petrolina, Brazil”. 08 Jul. 2017 <https://weatherspark.com/y/147603/Average-Weather-at-Petrolina-Brazil>.

Çengel, Y. A. and Ghajar, A. J., 2012. *Transferência de Calor e Massa*. AMGH, Porto Alegre, 4ª edição.

CEPEL, 2012. *Internal Report*. Rio de Janeiro, RJ, Brazil.

CoolProp, 2017. “CoolProp C++ Open-Source Thermophysical Property Library”. <http://www.coolprop.org>.

De Vos, A., 1992. “Endoreversible Thermodynamics of Solar Energy Conversion”. *Oxford Univ. Press*, Oxford.

Gilat, A., 2014. *MATLAB: An Introduction with Applications*. John Wiley & Sons, New York, 5th edition.

Jeter, S. M., 1981. “Maximum conversion efficiency for the utilization of direct solar radiation”. *Solar Energy*, Vol. 26, pp. 231-236.

Lazzaretto, A. and Tsatsaronis, G., 1999. “On the calculation of efficiencies and costs in thermal systems”. In *Proceedings of the ASME Advanced Energy Systems Division* (Aceves, S. M. *et al.*, eds.). AES-Vol. 39, p. 421-430. New York, NY.

Mahfuz, M. H., Kamyar, A., Afshar, O., Sarraf, M., Anisur, M. R., Kibria, M. A., Saidur, R. and Metselaar, I. H. S. C., 2014. “Exergetic analysis of a solar thermal power system with PCM storage”. *Energy Conversion and Management*, Vol. 78, pp. 486-492.

Microsoft, 2017. “COM: Component Object Model Technologies”. < https://www.microsoft.com/com/default.mspx >.
Nixon, J. D. and Davies, P. A., 2012. “Cost-exergy optimisation of linear Fresnel reflectors”. *Solar Energy*, Vol. 86, pp. 147-156.
Parrott, J. E., 1978. “Theoretical upper limit to the conversion efficiency of solar energy”. *Solar Energy*, Vol. 21, pp. 227-229.
Petela, R., 2003. “Exergy of undiluted thermal radiation”. *Solar Energy*, Vol. 74, pp. 469-488.
Petela, R., 1964. “Exergy of Heat Radiation”. *Journal of Heat Transfer* – Copyright by ASME, pp. 187-192.
Press, W. H., 1976. “Theoretical maximum for energy from direct and diffuse sunlight”. *Nature*, Vol. 264, pp. 734-735.
Reddy, V. S., Kaushik, S. C. and Tyagi, S.K., 2013. “Exergetic analysis and performance evaluation of parabolic dish Stirling engine solar power plant”. *International Journal of Energy Research*, Vol. 37, pp. 1287-1301.
SimTech, 2013. “IPSEpro Process Simulator – System Version 6.0”. Graz, Austria.
Spanner, D. C., 1964. *Introduction to Thermodynamics*. Academic Press, London, 1st edition.
Therminol Heat Transfer Fluids by Eastman Chemical Company or its subsidiaries, 2017. “Therminol® VP-1 Heat Transfer Fluid”. 08 Jul. 2017 <https://www.therminol.com/products/Therminol-VP1>.
Vieira, L. S., Donatelli, J. L. and Cruz, M. E., 2009. “Exergoeconomic improvement of a complex cogeneration system integrated with a professional process simulator”. *Energy Conversion and Management*, Vol. 50, pp. 1955-1967.
Wright, S. E., Rosen, M. A., Scott, D. S. and Haddow, J. B., 2002. “The exergy flux of radiative heat transfer for the special case of blackbody radiation”. *Exergy*, Vol. 2, pp. 24-33.
Xu, C., Wang, Z., Li, X. and Sun, F., 2011. “Energy and exergy analysis of solar power tower plants”. *Applied Thermal Engineering*, Vol. 31, pp. 3904-3913.

9. RESPONSIBILITY NOTICE

The authors are the only responsible for the printed material included in this paper.